Supplementary Information

Morphology Impact of Manganese-Cerium Oxides in Ethanol Oxidation

Huaju Li,[a] Gongshin Qi,[b] Tana,[a] Xiaojing Zhang,[a] Wei Li,*[b] and Wenjie Shen*[a]

[a] State Key Laboratory of Catalysis, Dalian Institute of Chemical Physics, Chinese Academy of Sciences, Dalian 116023, China

[b] General Motors Global Research and Development, Chemical Sciences and Materials Systems Lab, 30500 Mound Road, Warren, MI 48090, USA

Contents

Table S1 Structural parameters of the MnO_x-CeO_2 nanomaterials

Sample	2 theta (degree)	d (nm)	Crystalline size (nm)*	Lattice parameter (nm)
CeO_2	28.549	0.31240	-	0.54113
Nanocubes	28.565	0.31163	14.1	0.53975
Nanorods	28.571	0.31171	6.2	0.53990

*Calculated from the {111} diffraction line.

The MnO_x-CeO_2 oxides exhibited higher Bragg angles and lower lattice parameters than pure ceria, indicating the incorporation of manganese ions into ceria lattice.

Table S2 Surface compositions of the MnO_x-CeO_2 nanomaterials based on XPS analyses

Sample	Surface atom ratio (%)			Surface molar ratio (%)			$Ce^{4+}/(Ce^{4+}+Ce^{3+})$ (%)	$O_\alpha/(O_\alpha+O_\beta)$ (%)
	Mn	Ce	O	Mn^{4+}	Mn^{3+}	Mn^{2+}		
Nanocubes	6.3	27.2	66.5	25.7	28.1	46.2	95.0	86.8
Nanorods	7.7	21.1	71.2	43.8	38.9	17.3	91.1	75.6

The chemical formulas were $Mn_{0.19}Ce_{0.81}O_{1.99}$ for the nanocubes and $Mn_{0.27}Ce_{0.73}O_{2.47}$ for the nanorods and they were in good agreement with the ICP results, indicating the homogeneous dispersion of manganese and cerium ions in the MnO_x-CeO_2 nanomaterials.

Table S3 Hydrogen consumptions in the H_2-TPR profiles

Sample	Total H_2 (μmol H_2 g^{-1})	$MnO_2 \rightarrow Mn_2O_3$ (μmol H_2 g^{-1})	$Mn_2O_3 \rightarrow Mn_3O_4$ (μmol H_2 g^{-1})	$Mn_3O_4 \rightarrow MnO$ (μmol H_2 g^{-1})	$Ce^{4+} \rightarrow Ce^{3+}$ (%)
Nanocubes	687	106	179	122	10.6
Nanorods	1540	143	372	438	23.5

Table S4 Specific reaction rates of the {100} and {111} planes in ethanol oxidation

Temperature (K)	C_2H_5OH (10^{-2} μmol m^{-2} s^{-1})		CH_3CHO (10^{-2} μmol m^{-2} s^{-1})		CO_2 (10^{-2} μmol m^{-2} s^{-1})	
	{100}	{111}	{100}	{111}	{100}	{111}
443	3.69	1.73	3.52	1.60	0.12	0.09
453	5.36	2.57	5.05	2.34	0.24	0.19
463	8.04	4.09	7.42	3.62	0.53	0.43
473	9.43	4.82	8.53	4.03	0.74	0.65
483	13.39	6.15	11.61	4.74	1.57	1.30
E_a (kJ mol^{-1})	53.9 ± 1.6	55.7 ± 2.3	49.8 ± 1.7	48.2 ± 2.4	108.9 ± 2.2	116.4 ± 2.5

The tests were conducted at 443-483 K, and the conversion of ethanol was adjusted to below 15 % by adjusting the gas hourly space velocity in order to calculate the reaction rates under differential reactor conditions. The CO selectivity was lower than 3.0 % and no ethyl acetate was formed.

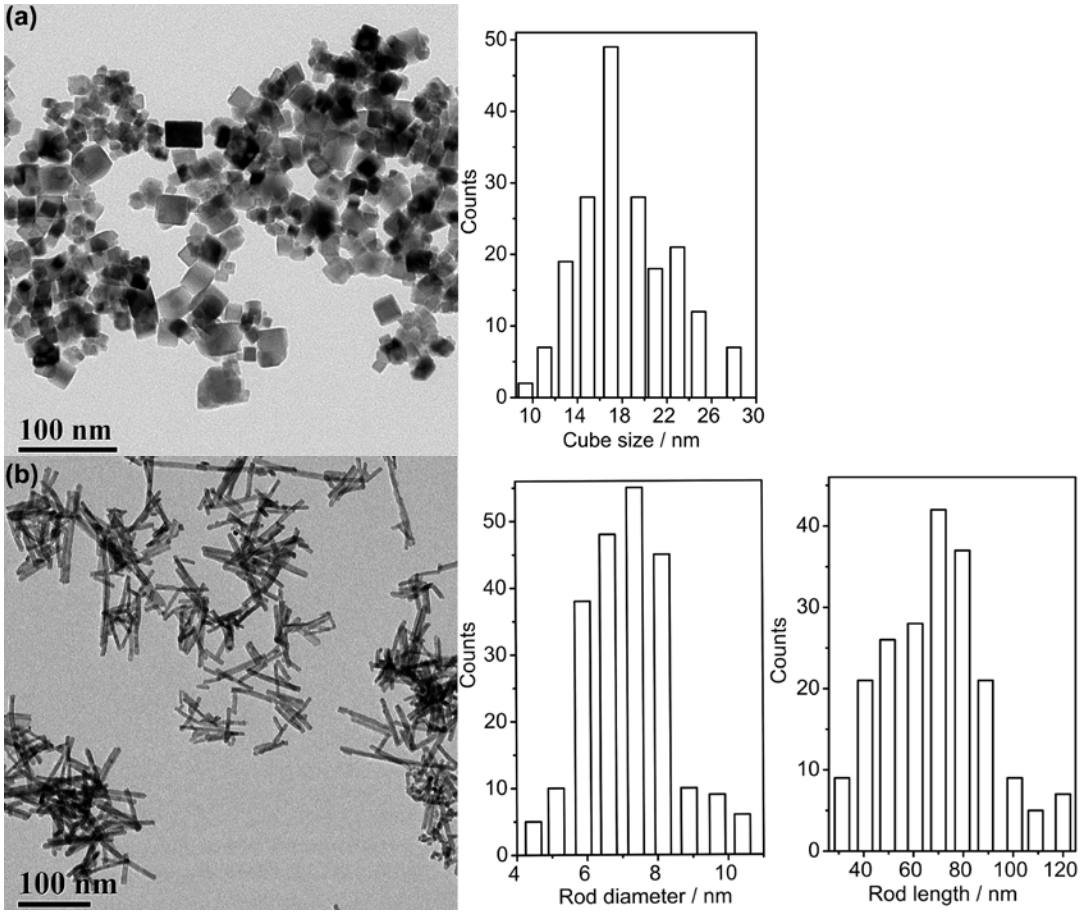

Fig. S1 TEM images and particle size distributions of MnO_x-CeO_2 nanocubes (a) and nanorods (b). By counting at least two hundred particles, the average particle size was 18 nm for the nanocubes, the average diameter was 7 nm and the mean length was about 70 nm for the nanorods (the aspectct ratio is about 10).

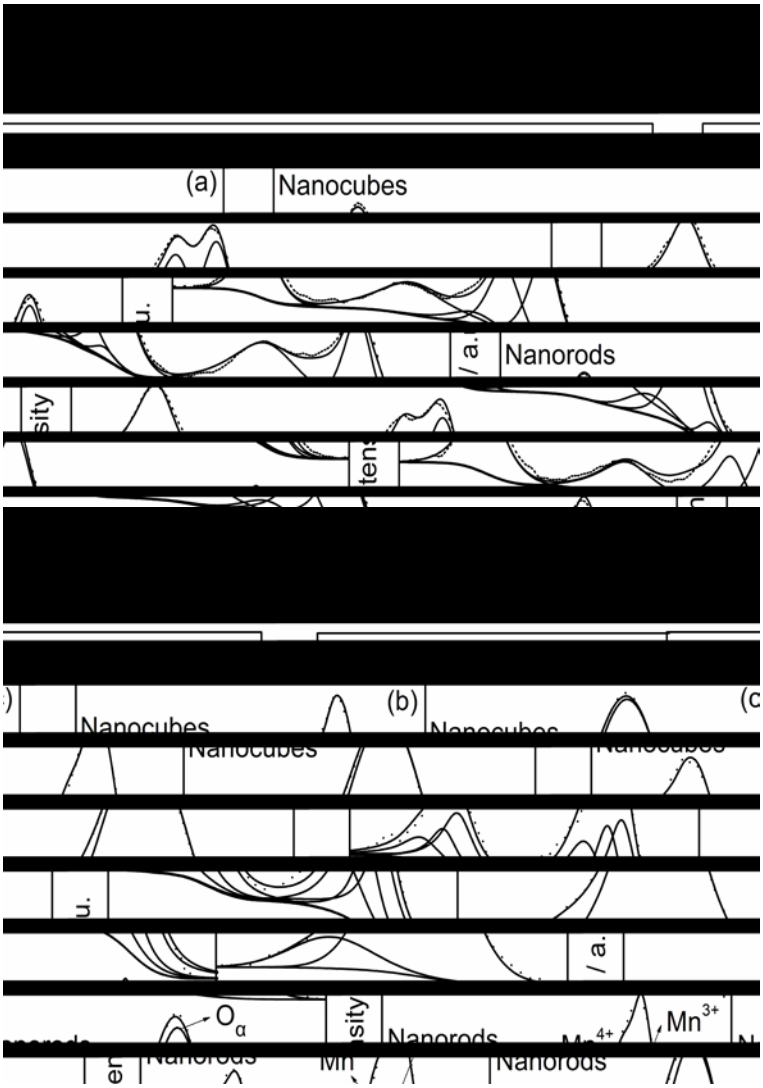

Fig. S2 XP spectra of Ce 3d (a), Mn 2p (b) and O 1s (c) of the MnO_x-CeO_2 nanomaterials. Quantitative analyses of Ce 3d profiles revealed that $Ce^{4+}/(Ce^{4+}+Ce^{3+})$ was 95.0 % on the nanocubes while 91.1 % on the nanorods (Table S2). The co-existence of Mn^{4+}, Mn^{3+} and Mn^{2+} species have been identified by the binding energies at 643.1, 642.6 and 641.5 eV, respectively. By deconvoluting the Mn 2p XP spectra, the average oxidation states of manganese were estimated to be 2.8 in the nanocubes and 3.3 in the nanorods. The O 1s spectra contained two types of oxygen species, the binding energy at 529.4 eV was assigned to the lattice oxygen (O_α) while the binding energy at 531.9 eV was attributed to oxygen species in the defects or hydroxyl-like groups (denoted as O_β). The nanocubes owned obviously more lattice oxygen than the nanorods.